J. Appl. Environ. Biol. Sci., 7(2S)37-44, 2017

ISSN: 2090-4274
Journal of Applied Environmental and Biological Sciences
www.textroad.com

One-Step Synthesis of Single Phase Rutile-Tianium Dioxide: Influence of Temperature on the Band Gap Energy

Evyan Yang Chia-Yan[1,2], Sarani Zakaria[1], Chin Hua Chia[1]

[1]School of Applied Physics, Faculty of Science and Technology, Universiti Kebangsaan Malaysia, 43600 Bangi, Selangor, Malaysia
[2]Department of Applied Sciences, Faculty of Science and Technology, Nilai University, 71800 Nilai, Negeri Sembilan, Malaysia

Received: February 21, 2017
Accepted: April30,2017

ABSTRACT

Single phase rutile titanium dioxides (TiO_2) nanocrystals have been synthesized via one-step hydrothermal method. The presence of hydrochloride (HCl) as a by-product during the hydrolysis played an important role in the growth of morphology and phase structure. The samples were calcined at 400°C, 500°C and 600°C to improve their crystallinity. The morphology and particle size were characterized using scanning electron microscopy (SEM), thermal electron scanning (TEM) and X-ray diffraction (XRD). Band gap energy (E_g) of the prepared rutile-TiO_2 were determined from the ultra violet-visible light (UV-vis) absorption spectra using Kubelka-Munk function, the values of E_g ranged from 2.75-3.2eV. From the study, the values of E_g decreased with increasing of temperature and particle size.

KEYWORDS: Rutile, Band Gap Energy, Hydrochloride (HCl), Kubelka-Munk Function.

INTRODUCTION

Titanium dioxide (TiO_2) is from the group of transition metal oxides which mostly appears naturally in three polymorphs, i.e. anatase (tetragonal), rutile (tetragonal) and brookite (orthorhombic). It broadly used as pigment in paints, cosmetics, papers and etc. It is extensively used as photocatalyst material [1-2]. Based on its high dielectric constant [3], it is also a popular dielectric material for photovoltaic cells [4-5]. In additional, TiO_2 can be applied in many other applications, such as gas purification, water filtration, sensor and medical supplication due to its high constancy, cost effectiveness and also safety to human and the environment.

Among the three polymorphs, rutile is the most thermodynamically stable phase. It shows a sufficient light-scattering effect without absorption virtually. Its band gap energy (~3.06eV) as a semiconductor is slightly lower than anatase (~3.23eV) [6]. Rutile is considered less active in photocatalytic activity if compared to anatase, which has dynamic charge carriers. However, rutile can be active or inactive in photocatalytic performance depending on the condition of preparation [7]. Apart from having suitable band gap energy, TiO_2 also possesses advantages, such as highly stable in aqueous media and non-toxic photocatalytic materials and etc. Anatase and brookite are in metastable form and can be readily transformed into rutile at high temperature [8-10]. Most of the studies reported that rutile-TiO_2 powders can be obtained by phase transformation from anatase phase through calcination at high temperature from 400°C or above [7, 9].

TiO_2 is commonly synthesized using sol-gel method or precipitation via hydrolysis in room temperature or higher temperature (thermohydrolysis). However, the precipitates of TiO_2 precursor obtained from these methods are in amorphous structure with anatase phase or mix phases of anatase and rutile. Calcination is needed to be carried out in order to attain crystalline products [10]. According to [11], there are many researchers work on synthesis and characterization of alkoxide-derived TiO_2 either in crystalline or amorphous. Although alkoxide precursors have been proven to synthesize TiO_2 with single phase anatase-TiO_2 or mix phases of anatase and rutile, the condition of producing must be under strict control because of its intense hydrolysis in the air [12,13]. On the other hand, several methods of synthesis TiO_2 are reported by adding reactant during precipitation of precursor with water or alcohol solution. The reactants including sodium nitrate [2], hydrogen peroxide [14], nitric acid [15] and ammonium sulphate [12], nevertheless, this could cause heterogeneity that extra steps are needed to produce the desired phases of TiO_2.

In present study, we have tried to optimize the preparation condition for producing single phase rutile-TiO_2 directly from simple and easy route. The band gaps related to the photocatalytic performance of TiO_2 and determined using Kubelka-Munk function.

Corresponding Author: Evyan Yang Chia-Yan, School of Applied Physics, Faculty of Science and Technology, Universiti Kebangsaan Malaysia, 43600 Bangi, Selangor, Malaysia, E-mail: evyanyang@nilai.edu.my

METHODOLOGY

Titanium tetrachloride, $TiCl_4$ (1.0M in methylene chloride, CH_2Cl_2, Sigma Aldrich) used as precursor due to its high reactivity in chemical reaction. The desired amount of $TiCl_4$ was added dropwise into a beaker containing deionized water. The volume ratio was set according to the reaction Equation(1) as the following:

$$TiCl_4 + 2H_2O \rightarrow TiO_2 + 4HCl \quad (1)$$

The solution left under vigorous stirring at room temperature for 40 minutes. The hydrolysis reaction started immediately upon mixing, which indicated by the formation of white flocs at the bottom of reaction beaker. The obtained solution transferred into a Teflon liner with capacity of 50ml and fit into stainless steel autoclave. The sealed autoclave was then put in oven for hydrothermal treatment at 180ºC for 24 hours. The product was collected by repeated washing with distilled water and ethanol, followed up by centrifugation in each washing. For comparison, two samples were prepared using hydrolysis method in room temperature for 24 hours and hydrothermal at 180ºC for 12 hours respectively.

The fine-powder from hydrothermal and hydrolysis was gained by freeze-drying overnight using freeze dryer (Scanvac Cool Safe -110-4). The freeze-dried samples prepared by hydrothermal for 24 hours were then thermal treated at 400ºC, 500ºC and 600ºC using furnace for further characterization.

The morphologies and the particle sizes of the synthesized powders were observed with Field Scanning Electron Microscopy (FESEM, Zeiss, SUPRA 55 VP) and TEM transmission electron microscopy (HD-2700 Cs-Corrected FE-STEM, Hitachi, Japan). The X-ray diffraction (XRD) patterns of the samples were obtained from X-ray diffractometer (Bruker Advance, USA) to identify the phase content of TiO_2. The crystallinities of the samples were determined using Bruker software namely Diffrac. eva. V4.0 (Bruker, England). The absorption spectra of the samples were collected using UV-vis NIR spectrophotometer (Lamba 950, Perkin Elmer, USA). Band gaps of the samples were defined and analysed by using Kubelka-Munk function.

RESULTS AND DISCUSSION

The powder which was prepared using hydrothermal method produced only rutile phase TiO_2 as shown in XRD pattern (Figure 1). Ti was hydrolyzed by OH group in the solvent (H_2O) and then crystallized TiO_2 were formed during thermal treatment for long hour [16].Unlike the results that reported by other researchers, anatase-TiO_2 particles or mixture of anatase- and rutile-particles were formed after thermal treatment in Teflon-lined autoclave [13, 17]. This could be affected by the interval time of thermal treatment up to 24 hours as compared to the study by [18], which the products were undergone hydrothermal for 15 hours. They were not able to get pure rutile phases by heating aqueous $TiCl_4$ solution from 80ºC-150ºC for maximum 15 hours unless increase the molarity of $TiCl_4$ to 1.2M.

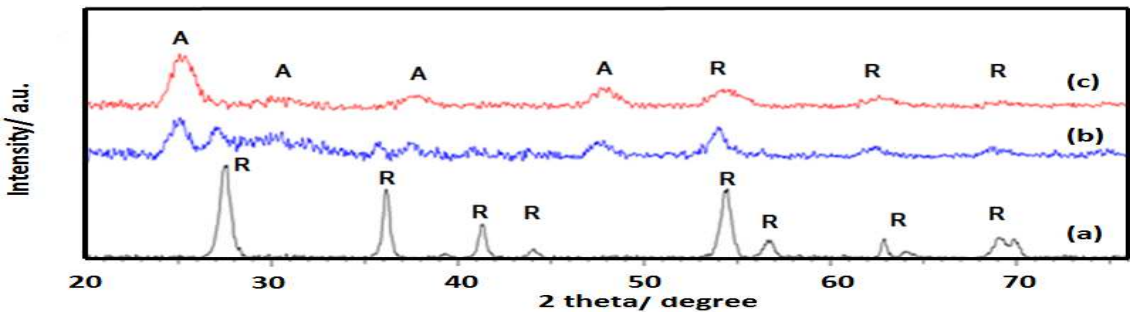

Figure 1: XRD patterns of TiO_2 powders which undergone (a) hydrothermal at 180ºC for 24 hours (b) hydrothermal at 180ºC for 12 hours and (c) hydrolysis at room temperature

The titanium precursor hydrolysed by water to produce TiO_2 and HCl gas released as the mole ratio of TiO_2 to HCl is 1:4. The dissolved HCl increased the acidity of the solution gradually during the hydrolytic process. As the reaction was seized in a closed autoclave system, it was high possibility that HCl gas could be dissolved and retained in the small stainless-steel reactor. Therefore, the acidity of the solution almost remained with averagely difference of pH value of 0.10 ± 0.01 before and after hydrothermal reaction. Rutile phase of TiO_2 preferable formed under higher concentration of HCl, while anatase or brookite phases of TiO_2 preferable formed under lower concentration of HCl [9, 19]. HCl as a by-product during the hydrolysis process plays an

important role as a built-in catalyst in stimulating the process by remaining or increasing the acidity level. In this case, the large amount of HCl retention promoted to rutile phase formation.

The basic structure units of all the TiO_2 crystal are in TiO_6 octahedrons which are similar to the microstructure of the TiO_2 crystals. For rutile, TiO_6 octahedrons form chain by edge-sharing along c axis then form three-dimension framework (3D) by corner oxygen atoms sharing to link the chains together (Figure 2(a)). For anatase, the 3D framework is formed by edge-sharing bonding among TiO_6 octahedrons as shown in Figure 2(b). Meanwhile, the formation of 3D framework for brookite is much complex with both corner- and edge-sharing bonding [20]. Therefore, it is easier to form either anatase or rutile. However, rutile is more thermodynamically stable if compared to anatase [11].

Figure 2: Two- dimensional projection of the TiO_6octahedra along c-axis in (a) anatase and (b) rutile (the bold lines refer to shared edges) [4]

Theoretically, phase transformation occurred when change in temperature or pressure or both. There was study on phase transition of TiO_2 based on high pressure in recent year [20]. Although liquid is incompressible, increasing of temperature will cause molecules of liquids tend to stay away from each other but this will be limited by the wall of the container. Therefore, pressure increase as well as the temperature increases. In current study, H_2O as a solvent undergone boiling continuously as the temperature reached 180^oC which was higher than the boiling point of H_2O (100^oC), thus, pressure in the autoclave reactor increased as explained. Eventually, TiO_2 rutile particles were obtained after 24 hours without further calcination. That is, phase transformation of anatase to rutile was expected to happen under the rapid boiling and sufficient high pressure within 24 hours. This situation was different from calcination which conducted at very high temperature (≥500^oC) within only short period of time (commonly, 2 hours). However, the autoclave system was not design to measure the pressure in the reactor thus two additional samples were synthesized with the same contents. One of the samples undergone hydrothermal treatment at180^oC for only 12 hours and another set was prepared using hydrolysis in room temperature for 24 hours. Both anatase- and rutile- TiO_2 were formed in these two samples as shown in XRD pattern of Figure 1(b) and 1(c). The results shown that penetration of H^+ and Cl^- can be carried out gradually under better controlled condition in the hydrothermal autoclave system to avoid heterogeneity caused by addition of reactant as discussed in the Introduction section.

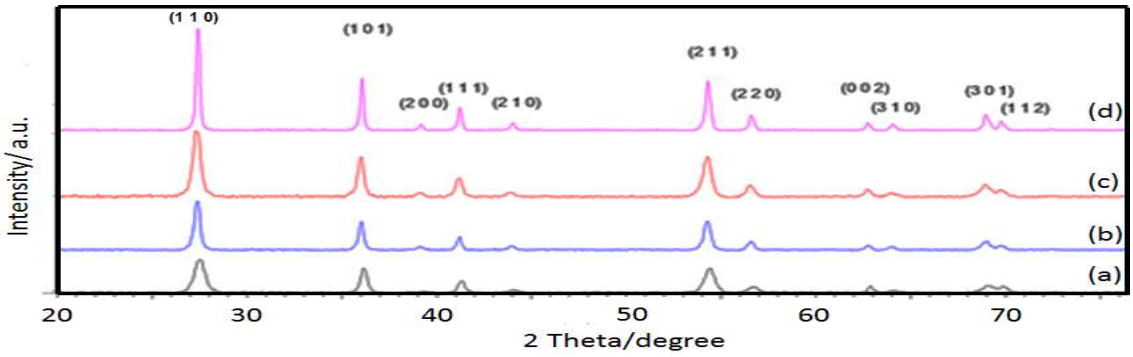

Figure 3: XRD patterns for samples that: (a) hydrothermal treated at 180^oC for 18 hours (b) calcined at 400^oC (c) calcined at 500^oC, and (d) calcined at 600^oC for 2 hours

The prepared samples were calcined at 400°C, 500°C and 600°C to check the crystallinity. Based on the XRD pattern in Figure 3, the phases for all the structure orientations were remained after calcination. This was proven stable crystal rutile-TiO_2 was formed directly after hydrothermal at 180°C for 24 hours. However, the crystallinity of the calcined sample was increased with the calcination temperature. According to the analysis of diffraction software (Bruker, England), the crystallinity for the sample after hydrothermal and calcination at 400°C, 500°C and 600°C were 67.8%, 72.1% and 82.4% respectively. The sizes of crystallites grew as the temperature increased.

From the SEM images in Figure 4, agglomeration was formed by rod-like particles. The rutile-phase nanoparticles were observed as short rod shape by some of the researchers [21] and this confirmed with the appearance of only rutile- peaks in XRD patterns. It was interesting to notice that the diameter and the length of the particles increased with increasing of thermal treatment temperature as shown in TEM pictures of Figure 5(a)-(d). This contributed to the increasing of peaks' intensities for the samples after calcination in XRD pattern (Figure 3). When temperature increased, the structure of TiO_2 particles became finer with the rearrangement of molecules. The thermodynamically stable rutile-TiO_2 could be rearranged in the intense structure. Meanwhile, the short bond length of TiO_6 octahedron formed longer chains in 3D framework thus the diameter and length of the rod-like particles averagely increased. Overall, the crystal sizes increased with the increase of particle sizes after the rearrangement of molecules during calcination. The average particle size for each sample was measured from the TEM images as 15.51nm, 27.22nm, 36.91nm and 50.81nm for samples before calcination, after calcination at 400°C, 500°C and 600°C respectively.

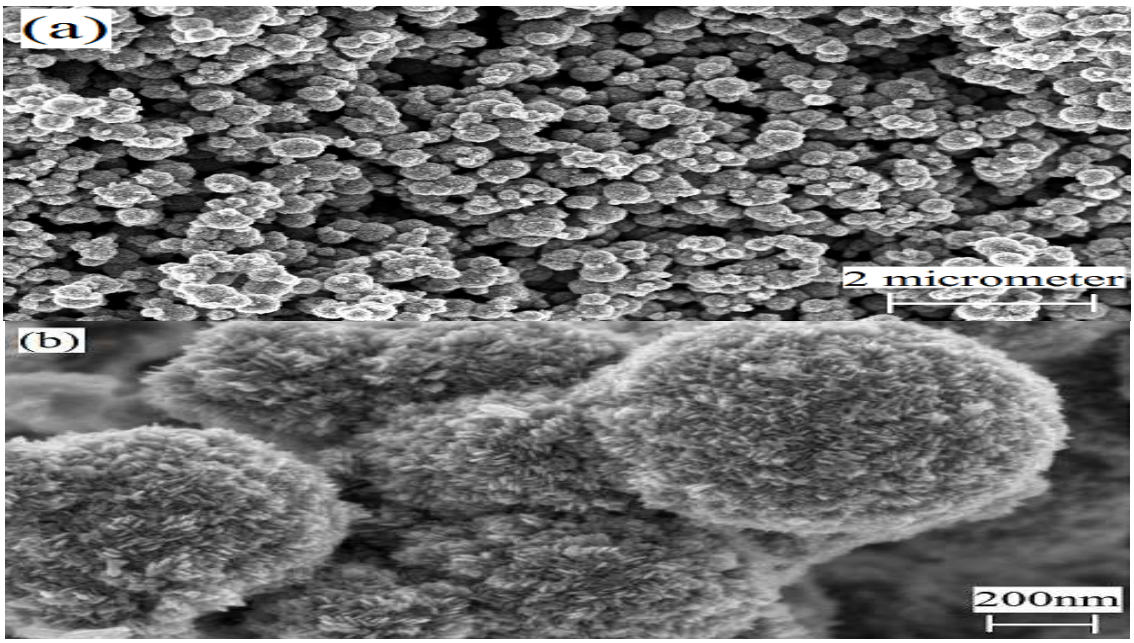

Figure 4: (a) TiO_2 powder from hydrothermal; (b) agglomeration of rod-like rutile-TiO_2

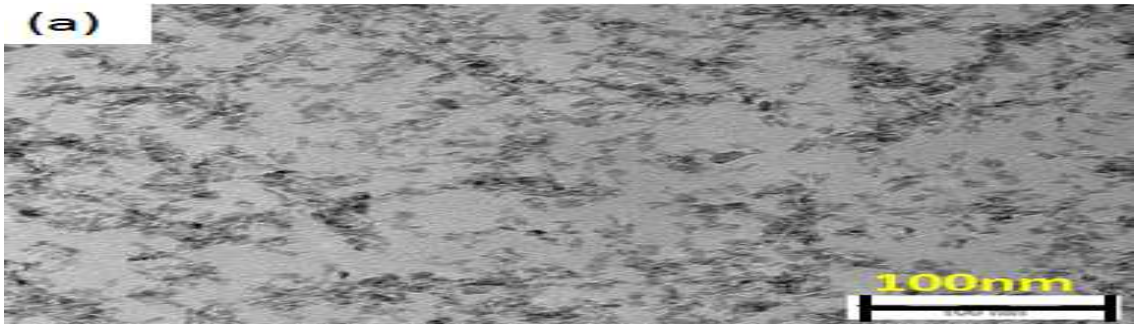

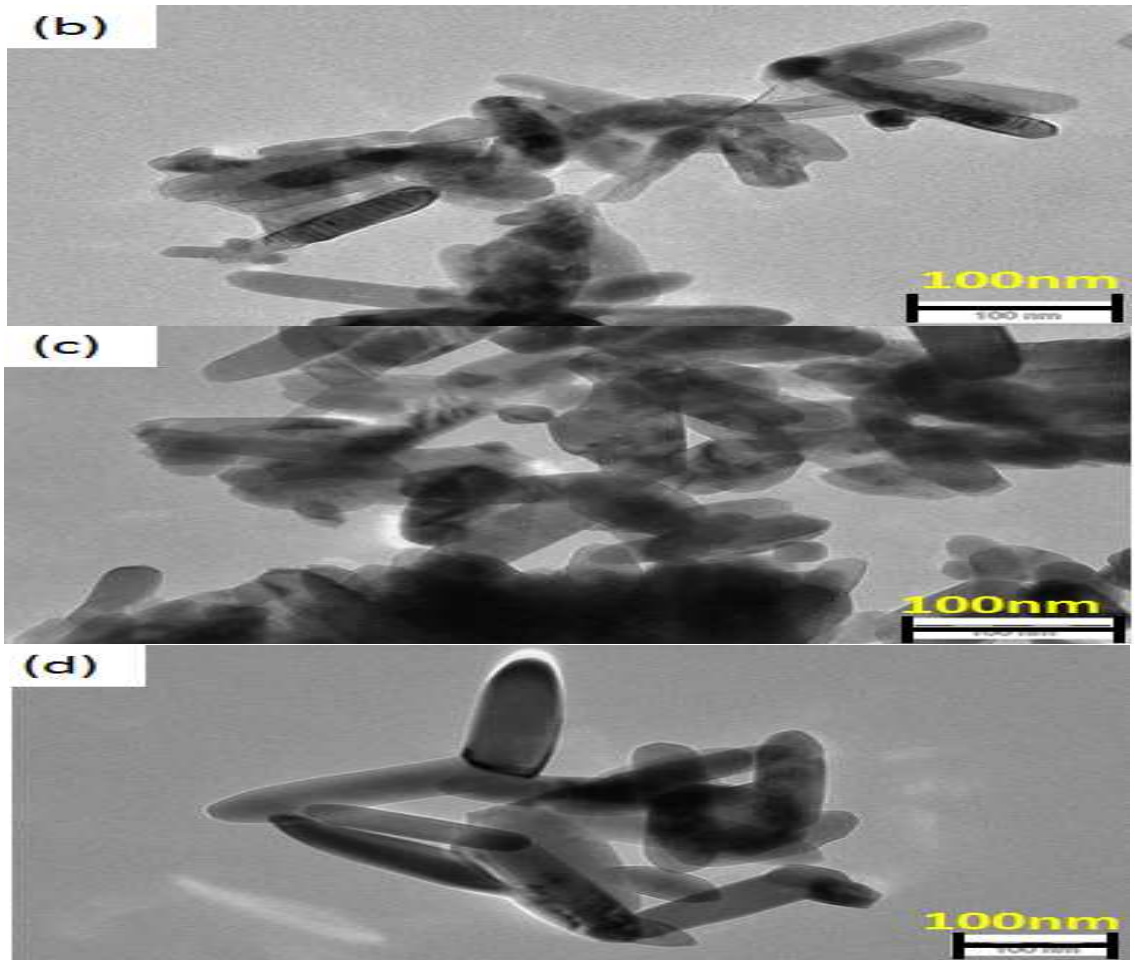

Figure 5: TEM images of the samples: (a) after hydrothermal; (b) after calcination at 400°C; (c) after calcination at 500°C; (d) after calcination at 600°C

The UV-vis absorption spectra of the samples displayed in Figure 6a. There were red-shifts of the absorption range to longer wavelength after the samples gone through calcination. The absorption tails extended close to 500 nm after thermal treatment at 400°C or higher temperature. Meanwhile, the spectrum of the sample that hydrothermal treated at 180°C corresponded more to the UV absorption with wavelength of 400 nm or less. This indicated that the rutile-TiO_2 of photocatalytic activity might be activated under visible light [8]. According to [21], the effect of amorphous content has been resulted in red shift of optical absorption band edge. However, this was not applicable on the current study as the synthesized powders were in rutile crystal after hydrothermal process. Conversely, another study by the same research group found that the quantum size effect on rutile-TiO_2 clusters was more obvious if compared to the same size of anatase-TiO_2 cluster [7, 10]. This is proven from the absorption spectra of the samples after calcination at different temperature. The crystallite sizes of the samples increased when the temperature increased as discussed in the previous section by measurement from Diffrac Eva. V4.0 software. The grain growth improved with the growth of crystallite size. Subsequently, the surface area enlarged with the rising of particle size. This prepared larger surface area for light absorption [22].

The band gap energy E_g can be determined by Kubelka-Munk function. The E_g for semiconductors is related to the optical absorption coefficient α with the following equation [23]:

$$\alpha h\upsilon = A(h\upsilon - E_g)^n \quad (2)$$

Where $h\upsilon$ = photon energy and A = constant that relative to the properties of the material.

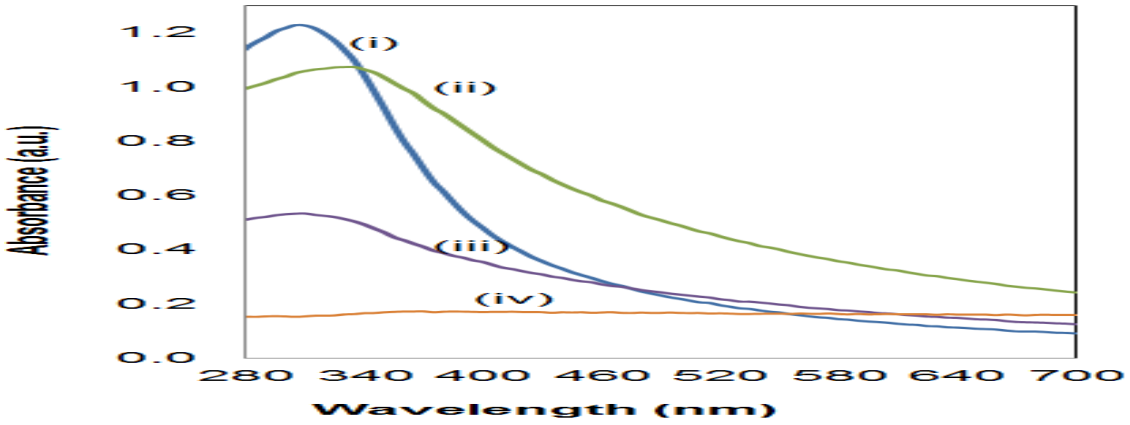

(a)

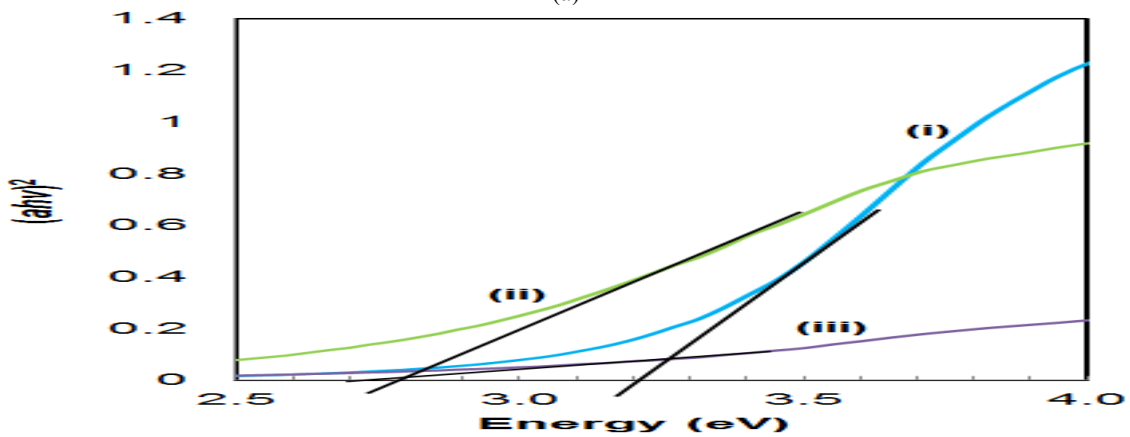

(b)

Figure 6: (a) UV-Vis spectra of TiO_2-rutile: (i) after hydrothermal (ii) after calcination at 400°C (iii) after calcination at 500°C and (iv) after calcination at 600°C. (b) Curve of $(\propto h\nu)^2$~ hvof TiO_2- rutile: (i) after hydrothermal (ii) calcination at 400°C (iii) calcination at 500°C

Refer to Equation (2), the value of n is 0.5 for direct allowed transition and n is 2 for indirect allowed transition whereas n = 1.5 for direct forbidden transition. The forbidden transitions will not be concerned in the study because it is very low probability to occur based on the symmetry rules [23]. For direct transition materials, the minimum in the conduction band(V_C) coincides with the maximum in the valence band(V_B) thus stimulating the return of the electron from V_C to V_B. For indirect transition materials, the minimum in V_C is apart from the maximum in V_B and this allows photoexcited electrons to remain at the lower energy level in V_C leading to a longer lifetime and greater mobility [24].

E_g of the crystalline semiconductor particles are depend on the particle size when the exciton radius is similar or higher than the particle size according to the Bohr's Model. The Bohr's exciton radius, a_B[17]:

$$a_B = \frac{\varepsilon h^2}{m_e^* e^2} \qquad (3)$$

The only phase occurred in the samples was rutile as confirmed with XRD pattern (Figure 3). Rutile has effective mass, m* of ~ $20m_e$ and permittivity, ε ~ 100 thus it a_B ~ 2.6Å[6]. In current study, the a_B of rutile was significantly smaller compared to particle size, this resulted in values of E_g depended on the particle size.

Rutile exhibited direct transition as suggested by most of the researchers [23-26]. This is in agreement with the estimated E_g values from the extrapolation of the linear part of the $\alpha h\upsilon \sim h\upsilon$ graph. The value of E_g for the sample before calcination is 3.20eV, meanwhile, E_g of the samples which calcined at 400°C and 500°C are 2.80eV and 2.75eV respectively. This could be attributed to the quantum size effects due to crystallite size [27]. The crystallinity increased with the calcination temperature which caused larger particle size as observed from the TEM images in Figure 5. That is, as the temperature increased, the absorption edge shifted to longer wavelength, consequently, band gap of the samples narrowed after calcination as shown in Figure 6b. The photocatalytic performance of rutile-TiO_2 is expected higher with lower E_g due to the direct transition of electrons in rutile, electrons are photoexcited directly to conduction band when gain enough energy. On the

other hand, the E_g of the sample after calcination at 600°C could not be estimated as its $\alpha h\upsilon \sim h\upsilon$ graph was distorted and not linear. The reading from the UV-Vis spectrometer for the sample calcined at 600°C was not consistent due to the large particle size that made the absorption inaccurate when dilute in distilled water as background solution. In addition, deep and shallow traps are created near the band edge by the defects in the bulk semiconductor due to delocalization of molecular orbitals on the surface. That is the irregular traps resulted in red-shift in absorption spectra and dropping of E_g values when the particle size increases with the temperature of heat treatment [28].

Although rutile with lower E_g is easily to be achieve excitation of electron to conduction band. However, the narrow band gap of rutile triggers recombination rate of holes and electrons higher than that of anatase. This is due to its shallow band bending in rutile, subsequently, only the holes that are closest to the surface will be trapped and transferred to the surface for redox reaction [29, 30]. Rutile has been proven to be additive to enhance the photocatalytic performance with single phase anatase TiO_2. This is caused by electron trapping site effectively interfacial charge transfer between anatase and rutile, which promote charge separation and hinder charge recombination as performed in commercial TiO_2 powder P-25 that consisted of anatase and rutile phases [31].

CONCLUSION

TiO_2 powder with single phase rutile is obtained from hydrothermal method using $TiCl_4$ as precursor and water as reactant. This method allows an approach which is simple and one-step. The key factors for determining morphology and crystal phases are the retention of HCl and long interval time of treatment. The by-product of HCl is acted as built-in catalyst which affected the formation of mechanism and crystal structures. This has lighted up a cost- effective method to prepare rutile-TiO_2.

The band gaps of the samples have been analysed based on Kubelka-Munk function. The average particle sizes of the rutile-TiO_2 are increased with increasing of calcination temperature and resulted in narrowing of band gaps. Thus, it is expected that the photocatalytic performance of the prepared rutile improved by increasing of calcination temperature.

ACKNOWLEDGMENT

The authors would like to express appreciation to Ministry of Higher Education Malaysia for the grant of LRGS/TD/2012/USM-UKM/PT/04, AP (2015-005), MyBrain scholarship and the funding by a research grant from Nilai University (MS006).

REFERENCES

1. Farhan, J.N., A.J. Aishah, T. Sugeng, R. Adnan and W.A. Mohamad. 2016. Significant Effect of PH on Photocatalytic Degradation of Organic Pollutants Using Semiconductor Catalysts. Jurnal Teknologi, 78 (8-3): 7-12.
2. Maulidiyah, M. N., W. Elsa A. Thamrin and W. Dwiprayogo, 2015. Preparation of Visible Photocatalyst N-TiO_2 and Its Activity on Congo Red Degradation. ARPN Journal of Engineering and Applied Sciences, 10 (15): 6250-6256.
3. Shankar, D., P. Ramjay and C. Ratnamala, 2015. Electrical Properties of Spin Coated Ultrathin Titanium Oxide Films on GaAs. Material Research Express, 2 (4): 1-8.
4. Dorian, A.H.H. and C.S. Charles, 2011. Review of the Anatase to Rutile Phase Transformation. Journal of Material Science, 46 (4): 855-874.
5. Ahmad, Z., M.S. Ghazali, H. Salleh, A. Zakaria, S. Mohd Ghazali, M.A. Zulkifliand M.E.A. Khamsan, 2016. The Conductivity Study of Hybrid Solar Cells of TiO_2 and Doped With Bixa Orellana for Solar Cells Application. Jurnal Teknologi (Sciences and Engineering), 78(3): 331-335.
6. Sergio, V., J. Miguel, and R. Gloria, 2010. Study of the Bandgap Synthesized Titanium Dioxide Nanoparticles Using the Sol-Gel Method and a Hydrothermal Treatment. The Open Material Science Journal, 4 (1): 9-14.
7. Gupta, S.M. and M. Tripathi, 2011. A Review of TiO_2 Nanoparticles. Chinese Science Bulletin, 56 (16): 1639-1657.
8. Mahshid, S., S.M. Ghamsari, M. Askari, N. Afshar and S. Lahuti, 2006. Synthesis of TiO_2Nanoparticles by Hydrolysis and Perpetuation of Titanium Isopropoxide Solution. Semiconductor Physics, Quantum Electronics and Optoelectronics, 9 (2): 65-68.
9. Paola, A.D., G. Cufalo, M. Addamo, M. Bellardita, R.Campostrini, M. Ischia, R. Ceccato and L. Palmisano, 2008. Photocatalytic Activity of NanocrystallineTiO_2 (Brookite, Rutile and Brookite-Based) Powders

Prepared by Thermohydrolysis of $TiCl_4$ in Aqueous Chloride Solutions. Colloids and Surface A: Physicochemical and Engineering Aspects, 317 (1-3): 366-376.
10. Chowdhury, M.M.I. and M.S. Vohra, 2016. Photocatalytic Degradation of Some Changes Aqueous Phase Pollutants Using Nafion and Silica Modified TiO_2. Sains Malaysiana, 45 (3): 477-487.
11. Joanna, M., Z. Anna, J. Marcin and H. Jan, 2016. The Effect of Calcination Temperature on Structure and Photocatalytic Properties of WO_3/TiO_2Nanocomposites. Journal of Nanomaterials, 2016: 1-9.
12. Gao, L. and Q.H. Zhang, 2001. The Promoting Effect of Sulfate Ions on the Nucleation of TiO_2 (Anatase) Nanocrystals. Materials Transactions, 42 (8): 1676-1680.
13. Payakgul, W., O. Mekasuwandumrong, V. Pavarajarn and P. Praserthdam, 2005. Effects of Reaction Medium on the Synthesis of TiO_2Nanocrystals by Thermal Decomposition of Titanium (IV) n-Butoxide. Ceramic International, 31 (3): 391-399.
14. Wu, X., E. Holbig and G. Steinle-Neumann, 2010. Structural Stability of TiO_2 at High Pressure in Density-Functional Based Calculations. Journal of Physics: Condensed Matter, 22 (29): 1-7.
15. Li, Q.J. and B.B. Liu, 2016. High Pressure Structural Phase Transition of TiO_2Nanomaterials. Chinese Physics B, 2016 (7): 22-30.
16. Macwan, D.P., N.D. Pragnesh and C. Shalini, 2011. A Review on Nano-Tio_2 Sol-Gel Type Syntheses and its Applications. Journal of Material Science, 46 (11): 3669-3686.
17. Nadtochenko V., N. Denisov, A. Gorenberg, Y. Kozlov, P. Chubukov, J.A. Rengifo, C. Pulgarin and J. Kiwi, 2009. Correlations for Photocatalytic Activity and Spectral Features of Absorption Band Edge of TiO_2 Modified by Thiourea. Applied Catalysis B: Environmental, 91 (1): 460-469.
18. Jeong, H.L. and S.Y. Yeong, 2005. Estimation of Reaction Conditions for Synthesis of Nanosized Brookite-Type Titanium Dioxide from Aqueous $TiOCl_2$ Solution. Journal of Materials Science, 40 (11): 2843-2847.
19. Wang, C., Z. Deng, X.S. Fan and Y. Li, 2002.Synthesis of Nanocrystalline TiO_2 in Alcohols. Powder Technology, 125 (1): 39-44.
20. Nyarkson, E., B. Agyei-Tuffour, J. Asare, E. Annan, E.R. Rwenyagila, D.S. Konadu and A. Yaya, 2013. Nanostructured TiO_2 and Their Energy Application-A Review. ARPN Journal of Engineering and Applied Sciences, 8 (10): 871-886.
21. Zhang, Q., L. Gao and J. Guo, 2000. Effects of Calcination on the Photocatalytic Properties of Nanosized TiO_2Powders Prepared by $TiCl_4$ Hydrolysis. Applied Catalysis B: Environmental, 26(3): 207-215.
22. Lu, C.H. and M.C. Wen, 2008. Synthesis of Nanosized TiO_2Powders via a Hydrothermal Microemulsion Process. Journal of Alloys and Compounds, 448(1): 153-158.
23. Khamsan, M.E.A., M. Ghazali, M. Sabri, H. Salleh, A. Zakaria, S. Mohd Ghazali, Z. Ahmad and M.S. Abd Aziz, 2016. Optical Characterization on ITO/TiO2/P3HT/Areca Catechu/Au for Thin Film Hybrid Solar Cell. Jurnal Teknologi (Sciences and Engineering), 78(3): 247-251.
24. Banerjee, S., J. Gopal, P. Muraleedharan, A.K. Tyagiand B. Raj, 2006. Physics and Chemistry of Photocatalytic Titanium Dioxide: Visualization of Bacterial Activity Using Atomic Force Microscopy. Current Science, 90 (10): 1378-1383.
25. Tariq, M., C.B. Cao, A. Rashid, A. Maqsood, M.A. Saeed, A.Z. Abrar, T. Husain and M.A. Kamran, 2013. Pressure Induced Structural and Electronic Bandgap Properties of Anatase and Rutile TiO_2. Sains Malaysiana, 42 (2): 231-237.
26. Saupe, G.B., Y. Zhao, J. Bang, N.R. Yesu, G.A. Carballo, R. Ordonez and T. Bubphamala, 2005. Evaluation of a New Porous Titanium-Niobium Mixed Oxide for Photocatalytic Water Decontamination. Microchemical Journal, 81(1): 156-162.
27. Lin, H., C.P. Huang, W. Li, C. Ni, S. Ismat Shah and Y.H. Tseng, 2006. Size Dependency of Nanocrystalline TiO_2 on its Optical Property and Photocatalytic Reactivity Exemplified by 2-Chlorophenol. Applied Catalysis B: Environmental, 68 (1): 1-11.
28. Li, G., L. Chen, M.E. Graham and K.A. Gray. 2007. A Comparison of Mixed Phase Titania Photocatalysts Prepared by Physical Solid-Solid Interface. Journal of Molecular Catalysis A: Chemical, 275 (1-2): 30-35.
29. Meulen, T.V.D., A. Mattson and L. Osterlund, 2007. A Comparative Study of the Photocatalytic Oxidation of Propane on Anatase, Rutile and, Mixed-Phase Anatase-Rutile TiO_2Nanoparticles: Role of Surface Intermediates. Journal of Catalysis, 251 (1): 131-141.
30. Hurun, D.C., A.G. Agrious, K.A. Gray, T. Rajih and M.C. Thurnaur, 2003. Explaining the Enhanced Photocatalytic Activity of Degussa P-25 Mixed Phase TiO2 Using EPR. Journal of Physics and Chemistry B, 107 (19): 4545-4549.
31. Mohamad, A.M., W.N.W. Norharyati, J. Juhana and Y. Norhaniza. 2014. Preparation and Photocatalytic Activity of Mixed Phase Anatase/Rutile TiO_2Nanoparticles for Phenol Degradation. Jurnal Teknologi, 70(2): 65-70.